

Tape transport control based on sensor fusion

Angeliki Pantazi*, Giovanni Cherubini*, Eiji Ogura**, and Jens Jelitto*

**IBM Research – Zurich, 8803 Rüschlikon, Switzerland
(e-mail: {agp, cbi, jje}@zurich.ibm.com)*

***IBM STG, Tokyo, Japan (e-mail: eogura@jp.ibm.com)*

Abstract: Reliable and precise tape transport is of fundamental importance to achieve larger volumetric recording densities in tape storage systems. The performance of the tape transport control system, which is affected by variations in the tape velocity and tension, impacts the write and read quality of the data tracks and eventually the achievable areal recording density. During operation in cruise velocity mode, disturbances in velocity and tension may be induced for example by tape reel eccentricities. This problem is particularly serious when the reel rotation frequencies are close to the resonance frequency determined by the tape path. Typically, the tape velocity is estimated at the tape head from a servo signal, which is obtained by reading pre-formatted servo information, and used for tape transport control during cruise mode. In such a scheme, velocity disturbances observed at the head cannot be attributed to an individual reel. Hence no targeted disturbance suppression can take place at the individual tape reels. However, Hall sensors are typically included in tape drives to obtain additional tape velocity information from the individual reels. This information is used to achieve proper tape transport operation in the absence of valid velocity estimates from the pre-formatted servo information, for example during tape acceleration. In this paper, we present a novel control scheme for tape transport that uses velocity measurements from three sources, the Hall sensors at the tape reels and the servo channel that yields velocity estimates at the head. Specifically, characterization of the multiple-input multiple-output (MIMO) tape transport system provides an accurate system model and enables an optimized two-sensor control design. Furthermore, H_∞ filtering is employed to perform sensor fusion and the resulting state estimates are used in the feedback control of the two reels. Experimental results are presented to illustrate the behavior and performance of the proposed tape transport control system.

Keywords: Tape transport, velocity control, sensor fusion, MIMO system.

1. INTRODUCTION

The continuous growth of digital data – the International Data Corporation (IDC, 2012) projects the digital universe to grow to 40 zettabytes by 2020 – will require further drastic improvements of affordable and high capacity storage technologies to hold these vast amounts of data. Tape systems keep serving as a low cost storage tier by providing the lowest total cost of ownership and are especially suited for infrequently accessed data such as backup and archival storage (Reine and Kahn, 2010). Tape product roadmaps as well as the tape storage roadmap set by the Information Storage Industry Consortium (INSIC, 2012) indicate that extremely high tape capacities of more than 100 Tbyte appear feasible within the next decade. The potential for further significant tape areal density improvements have also been investigated in Argumedo et. al. (2008) and Cherubini et. al. (2011). Advances in several technology areas are necessary to achieve the aggressive tape capacity targets. Linear and track density increases as well as thinner tape media are key ingredients to achieving higher storage capacities.

In this paper we focus on the design of an improved reel-to-reel system to enable higher track density and to support thinner tape media through ultra-precise control of the tape-

transport system. In particular, tight control of velocity, tension and potentially of tape dimensional stability (TDS) variations will gain in importance when moving to thinner tape material in order to enable increased tape volumetric density.

In a conventional tape-transport system several sensors are used to determine the tape-transport parameters. Typically a primary tape velocity estimate is provided by reading a preformatted servo pattern from the tape with one or more servo readers and extracting the relevant information using a servo channel. The primary tape velocity provides a measure of the tape velocity at the tape head location. The limitation of sensing the primary velocity at the tape head is that velocity disturbances cannot be attributed to an individual tape reel. However, additional Hall sensors are available and are used to obtain secondary tape-velocity information from the individual reels. This information is typically more noisy than the primary velocity estimate, and is used to control the tape-transport operation in the absence of primary velocity estimates, e.g. during tape acceleration or deceleration or whenever the servo readers are not aligned with the servo patterns on tape.

The primary velocity response is typically assumed to be the average of the velocity responses at the two reels (Mathur

and Messner, 1998). With this approach, no targeted disturbance suppression is possible at the individual tape reels. However, a recent tape transport system identification study has shown that the primary tape velocity measured at the head is dominated by the velocity at the reel supplying the tape rather than by the average velocity of the supply and take-up reels (Cherubini et al., 2013).

In this paper, a novel tape transport control system is proposed, which exploits the availability of multiple sensors for velocity estimation and uses a sensor fusion approach that combines primary and secondary velocity estimates to optimally control the individual tape reels. First, the tape transport system identification procedure as developed in Cherubini et al. (2013) is briefly described. Measurements of the secondary tape velocities at the individual reels using Hall sensors and the primary velocity at the tape head are used for characterizing the relationships between the individual velocity contributions. It will be shown that the velocity observed at the head is essentially determined by the reel supplying the tape. Based on these findings, the classical tape transport system, which uses the primary velocity estimate to control both tape reels, will be extended. In a first approach, the take-up reel will be controlled by the Hall velocity measured at that reel, and the supply reel will be controlled by the primary velocity estimate. In a second approach, sensor fusion is introduced to optimally control the supply reel using both the primary velocity estimate and the Hall velocity estimate from the supply reel. The concept of sensor fusion has been successfully used for nanopositioning in probe storage devices (Pantazi et al., 2007). A detailed description of the concepts and controller design for nanopositioning with multiple sensors can be found in Sebastian and Pantazi (2012). In a tape reel-to-reel control system, sensor fusion can be used to combine the low-noise primary velocity estimate at the tape head with the more noisy measurement at the tape reels using Hall sensors, which however contain only reel-specific velocity components. The primary velocity estimates provide better noise performance compared with the Hall sensor measurements especially at high frequencies. The sensor fusion problem formulation is introduced, where the state variable of interest is the supply reel velocity. An H_∞ filtering approach is used for the estimator design. The optimal state estimate is obtained from the control signals and the measurements from the two sensors, i.e., the Hall sensor and the servo channel. Experimental results show that the concept of sensor fusion yields improved performance in terms of velocity variation and tape tension variation, especially mitigating disturbances close to the tape path resonance frequency.

The paper is organized as follows. The tape-transport system identification procedure is described in Section 2. Tape transport control by velocity feedback is introduced in Section 3 and extended with the concept of sensor fusion in Section 4. Experimental results are discussed in Section 5. The paper concludes with Section 6.

2. TAPE TRANSPORT SYSTEM IDENTIFICATION

The block diagram of the tape transport and track-following servomechanisms in a tape drive is shown in Fig. 1. For motion in the forward direction, the tape is transported from the file reel, acting as a supply reel, to the machine reel, acting as a take-up reel, through the tape path determined by the rollers R1 to R4. In reverse direction, the roles of the file reel and machine reels are reversed. Read/write operations are performed in contact with the tape by the read/write elements for the servo and data channels that are present in the tape head. A digital servo channel provides estimates of the tape velocity, tape longitudinal position, and head lateral position with respect to the tape, which are derived from servo signals that are read by servo readers in the head module. Hall sensors are used to obtain additional tape velocity information from the individual reels, which typically is used to achieve proper tape transport operation in the absence of valid parameter estimates from the servo channel, e.g., during tape acceleration. A servomechanism is considered here with no feedback of tension.

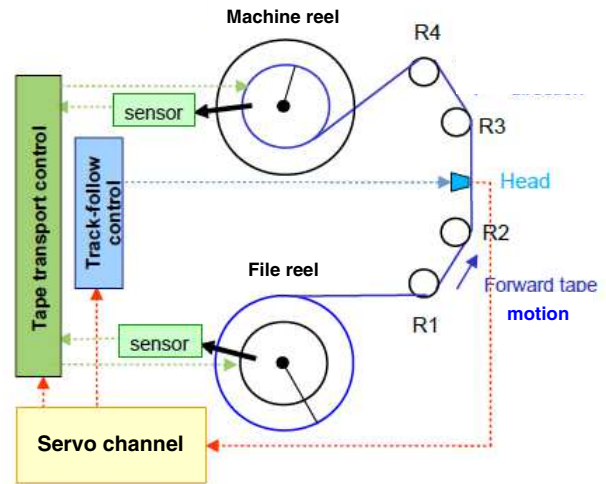


Fig. 1. Block diagram of tape transport and track-following servomechanisms.

A brief overview is now given of the tape transport model and identification method, described in detail in Cherubini et al. (2013). The mechanical behavior of the system is governed by second-order differential equations, which are obtained by equating the change in angular momentum to the sum of torques for each reel, and are expressed in state-space form as

$$\dot{\mathbf{x}}(t) = \mathbf{F} \mathbf{x}(t) + \mathbf{G} \mathbf{u}(t), \quad (1)$$

where the state vector is given by

$$\mathbf{x}(t) = \begin{bmatrix} x_m(t) \\ v_m(t) \\ x_f(t) \\ v_f(t) \end{bmatrix} = \begin{bmatrix} \text{tape position at machine reel} \\ \text{tape velocity at machine reel} \\ \text{tape position at file reel} \\ \text{tape velocity at file reel} \end{bmatrix}, \quad (2)$$

the vector of control signals is

$$\mathbf{u}(t) = \begin{bmatrix} u_m(t) \\ u_f(t) \end{bmatrix}, \quad (3)$$

and

$$\mathbf{F} = \begin{bmatrix} 0 & 1 & 0 & 0 \\ -(1+\mu)R_m^2K_T & -(1+\mu)R_m^2D_T - \beta_m & (1+\mu)R_m^2K_T & (1+\mu)R_m^2D_T \\ J_m & J_m & J_m & J_m \\ 0 & 0 & 0 & 1 \\ R_f^2K_T & R_f^2D_T & -R_f^2K_T & -R_f^2D_T - \beta_f \\ J_f & J_f & J_f & J_f \end{bmatrix}$$

$$\mathbf{G} = \begin{bmatrix} 0 & 0 \\ R_m K_m & 0 \\ J_m & 0 \\ 0 & 0 \\ 0 & R_f K_f \\ J_f & J_f \end{bmatrix}, \quad (4)$$

where K_T and D_T are the tape spring constant and damper coefficient, K_m and K_f are the motor driver gains, β_m and β_f are the motor viscous friction coefficients, R_m and R_f are the radii, J_m and J_f are the moments of inertia of the machine reel and file reel, respectively, and μ is the Coulomb friction coefficient. Note that the radii and the moments of inertia are time varying. The tape transport output signals are expressed for forward tape motion in terms of the state vector as

$$\mathbf{y}(t) = \begin{bmatrix} v_m(t) \\ v_f(t) \\ \tau \end{bmatrix} = \mathbf{H}\mathbf{x}(t), \quad (5)$$

where

$$\mathbf{H} = \begin{bmatrix} 0 & 1 & 0 & 0 \\ 0 & 0 & 0 & 1 \\ K_T & D_T & -K_T & -D_T \end{bmatrix},$$

and where $v_m(t)$ and $v_f(t)$ are the tape velocities at the machine and file reels, respectively, and $\tau(t)$ represents the tape tension. With reference to Fig. 1, the secondary velocities at the machine and file reels, $v_{H,m}(t)$ and $v_{H,f}(t)$, are measured by the Hall sensors, whereas the primary velocity $v(t)$ at the head is estimated by the servo channel.

System identification is performed in the frequency domain. The tape transport parameter estimates and the frequency responses of the tape transport system as described by Eqs. (1) to (5) are obtained at a given longitudinal tape position by alternatively superimposing chirp signals on the machine reel and file reel motor input signals, while the tape transport servomechanism is operated in closed loop at a certain nominal tape velocity and tension. Closed-loop operation during application of the chirp signals is considered to prevent large deviations of the regulated variables from the nominal values. The parameter values depend on longitudinal tape position, tape velocity, and tension, and are identified by the minimization of a cost function, which is given by the L_2 norm of the difference between the frequency responses of the system given by Eqs. (1) to (5) and those obtained by experimental waveforms.

For a wide range of tape velocities and tensions, the frequency responses from the input signals to the primary tape velocity closely match the responses from the input

signals to the secondary tape velocity at the supply reel, which is the file reel for tape motion in the forward direction, and the take-up reel in the reverse direction. This result indicates that in steady state, contrary to the assumption usually made that the primary velocity response is the average of the velocity responses at the individual reels, see, e.g., Mathur and Messner (1998), the primary tape velocity matches the secondary tape velocity at the supply reel. Figure 2 shows the frequency responses identified and the frequency responses obtained from the state-space model by substituting the estimated values of the parameters K_T and D_T in the model of Eqs. (1) and (5), for nominal values of tape velocity equal to 4.1 m/s and for a longitudinal position corresponding to the beginning of tape with motion in forward direction. The comparison of the frequency responses from the input signals to the primary velocity and to the Hall velocities indicates that the frequency responses from the input currents to the primary velocity closely match those from the input currents to the Hall velocity at the file reel, which for the considered case of forward tape motion plays the role of the supply reel, as mentioned above, whereas there is no match between the primary velocity and the Hall velocity at the machine reel.

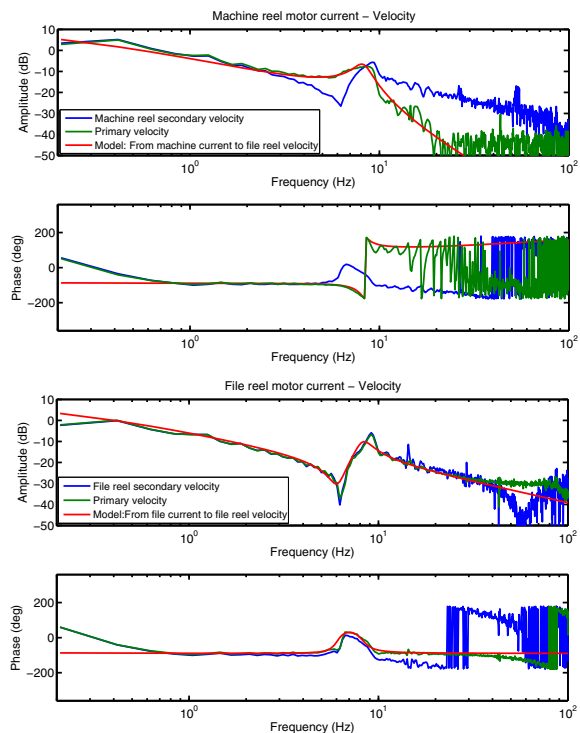


Fig. 2. Frequency responses from machine reel motor current to the primary and machine reel tape velocities (top), and from file reel motor current to the primary and file reel tape velocities (bottom), from Cherubini et al. (2013).

3. CONTROL OF TAPE TRANSPORT BY VELOCITY FEEDBACK

The block diagram of a classical tape transport control system with feedback of primary velocity is shown in Fig. 3. The closed-loop system for each reel consists of a feedback controller for tape-velocity control and a feedforward controller for tape-tension control. Fig. 4 illustrates the

spectrograms of the secondary and primary velocity measurements with tape motion in forward direction. Large spectral components are shown as dark red curves, whereas small spectral components are shown in light green. Note that the frequencies of the spectral components of the velocity at the machine reel, acting as take-up reel, decrease with time, as the machine reel radius increases, whereas the frequencies of the spectral components of the velocity at the file reel, acting as supply reel, increase with time. More importantly, the frequencies of the spectral components of the primary velocity tend to increase, indicating the strong coupling of the velocity at the file reel, or in general at the supply reel, with the primary velocity. Furthermore, this suggests that using the feedback of the primary velocity to control the velocity at both reels may lead to larger adjustment errors as compared to a control scheme where the coupling of primary and secondary velocity is taken into account.

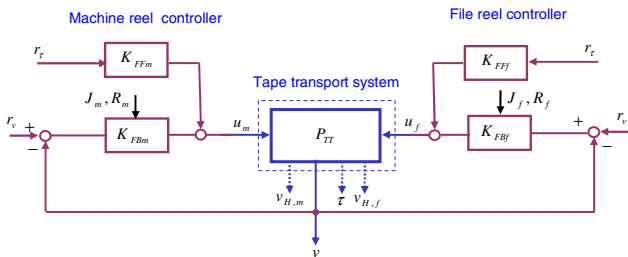


Fig. 3. Block diagram of tape transport control system with feedback of primary velocity.

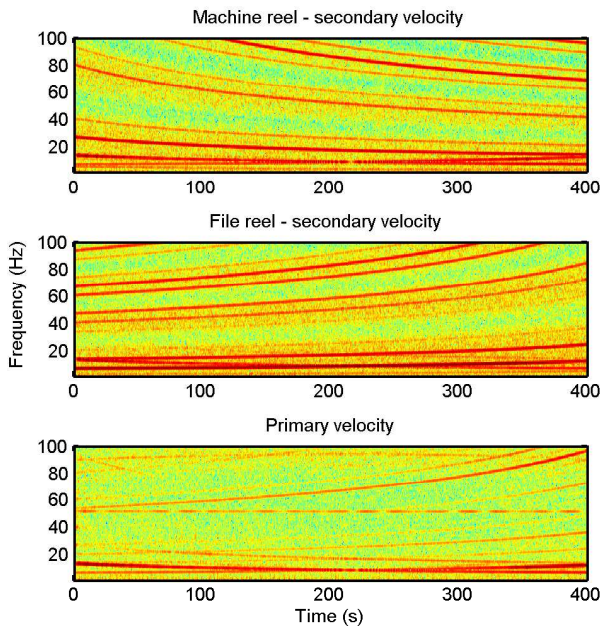


Fig. 4. Spectrograms of the secondary (top and middle) and primary (bottom) velocity measurements.

4. CONTROL OF TAPE TRANSPORT BASED ON SENSOR FUSION

The system identification and the velocity disturbance characterization presented in the previous sections have shown that there is no match between the primary velocity and the velocity measurement obtained by the Hall sensor at the take-up reel. Based on the above observation, the classical tape transport control system is modified as shown in the block diagram of Fig. 5. For the take-up reel the velocity feedback is yielded by the velocity measurement obtained by the Hall sensor at that reel.

For the supply reel, two approaches are considered. In the first approach, the primary velocity measurement is used directly for feedback control of the supply reel. Therefore, depending on the direction of tape motion a simple switching is performed in the velocity used for feedback control between the primary and the secondary measurements. In the second approach, sensor fusion is performed to obtain an optimal estimate of the supply reel velocity. The estimate of this state variable is subsequently employed for feedback control of the supply reel.

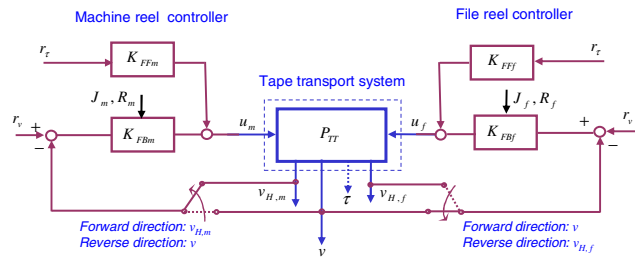


Fig. 5. Block diagram of tape transport control system with feedback of secondary and primary velocities.

Even though the identification results have shown that both the primary velocity estimated by the servo channel and the secondary velocity measured by the Hall sensor provide a good estimate of the velocity at the supply reel, a more accurate estimate of the velocity at the supply reel can be obtained by combining the information from both sensors. The primary velocity estimation is derived by accurate servo information formatted in the tape that is read by a servo reader and subsequently processed by the servo channel. Therefore primary velocity estimates have better noise performance than the Hall sensor measurements, especially at the high frequencies. However, the primary velocity is obtained when the tape reaches the head location, hence low-frequency velocity variations at the supply reel may not be accurately captured. Furthermore, as mentioned earlier, primary velocity is not available at very low speeds and during acceleration. Hence, it is essential to have the Hall velocity measurements always available, in addition to the primary velocity.

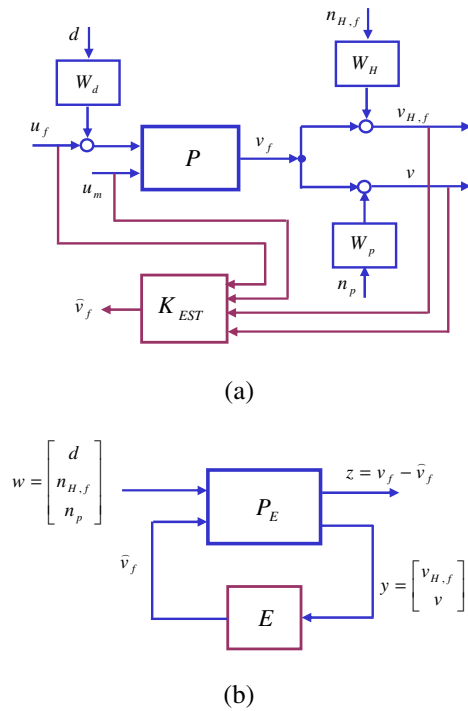


Fig. 6. Sensor fusion problem: block diagram representation (a), and LFT formulation (b).

A block diagram representation of the sensor fusion problem is illustrated in Fig. 6(a). An optimal estimate of the reel velocity state variable has to be obtained using an estimator K_{EST} . The relevant spectral characteristics of measurement noise sources and disturbances are captured by the weighting filters W_H , W_p and W_d having specific frequency responses. In particular, W_p is chosen to be a first order low-pass filter to capture inaccuracies of the primary velocity estimate at very low frequencies. For simplicity, W_H and W_d are chosen as scalar gains. The gain selection of the W_H weight aims at achieving a frequency separation of the two velocity measurements in the velocity estimate. Filter selection with more elaborate spectral shaping is possible, but will result in a higher-order estimator. The magnitude responses of the weighting filters for the noise sources are shown in Fig. 7. The W_d weight captures the characteristics of the disturbances that are assumed to be white. The augmented state-space equations describing the dynamics of the tape transport system including the weighting filters are given by

$$\begin{bmatrix} \dot{x}_m \\ \dot{v}_m \\ \dot{x}_f \\ \dot{v}_f \\ \dot{x}_p \end{bmatrix} = \begin{bmatrix} \overbrace{F_{11} & F_{12} & F_{13} & F_{14}}^A & 0 \\ F_{21} & F_{22} & F_{23} & F_{24} & 0 \\ F_{31} & F_{32} & F_{33} & F_{34} & 0 \\ F_{41} & F_{42} & F_{43} & F_{44} & 0 \\ 0 & 0 & 0 & 0 & A_p \end{bmatrix} \begin{bmatrix} x_m \\ v_m \\ x_f \\ v_f \\ x_p \end{bmatrix}$$

$$\begin{bmatrix} G_{11} & G_{12} \\ G_{21} & G_{22} \\ G_{31} & G_{32} \\ G_{41} & G_{42} \\ 0 & 0 \end{bmatrix} \begin{bmatrix} u_m \\ u_f \end{bmatrix} + \begin{bmatrix} \overbrace{G_{12}D_d}^{B_d} & 0 & 0 \\ \overbrace{G_{22}D_d}^{B_n} & 0 & 0 \\ \overbrace{G_{32}D_d}^{B_n} & 0 & 0 \\ \overbrace{G_{42}D_d}^{B_n} & 0 & 0 \\ 0 & 0 & B_p \end{bmatrix} \begin{bmatrix} d \\ n_H \\ n_p \end{bmatrix}$$

$$\begin{bmatrix} v_{H,f} \\ v \end{bmatrix} = \begin{bmatrix} \overbrace{0 & 0 & 0 & 1}^C & 0 \\ 0 & 0 & 0 & 1 & C_p \end{bmatrix} \begin{bmatrix} x_m \\ v_m \\ x_f \\ v_f \\ x_p \end{bmatrix} + \begin{bmatrix} \overbrace{0 & D_H}^{D_n} & 0 \\ 0 & 0 & D_p \end{bmatrix} \begin{bmatrix} d \\ n_H \\ n_p \end{bmatrix}$$

where F , G , denote the state-space matrices of the tape transport system P defined in Eq. 4, and A_p , B_p , C_p and D_p are the state-space matrices of W_p ; D_H and D_d are the constant gains of W_H and W_d , respectively.

For sensor fusion, the state variable of interest is the supply reel velocity, which corresponds to the file reel velocity for the considered case of forward direction of tape motion. An H_∞ filtering approach is used for the estimator design. The optimal state estimate is obtained from the control signals and the measurements from the two sensors, i.e., the Hall sensor and the servo channel. A linear fractional transformation (LFT) formulation of the sensor fusion problem is illustrated in Fig. 6(b). The generalized plant model is given by

$$P_E = \left[\begin{array}{c|cc} A & B_n & 0 \\ \hline C_1 & 0 & -I \\ C & D_n & 0 \end{array} \right]$$

where $C_1 = [0 \ 0 \ 0 \ 1 \ 0]$. The objective of the optimization problem is to design the estimator E such that it bounds the infinity norm of the transfer function $T_{zw} = F_l(P_E, E)$.

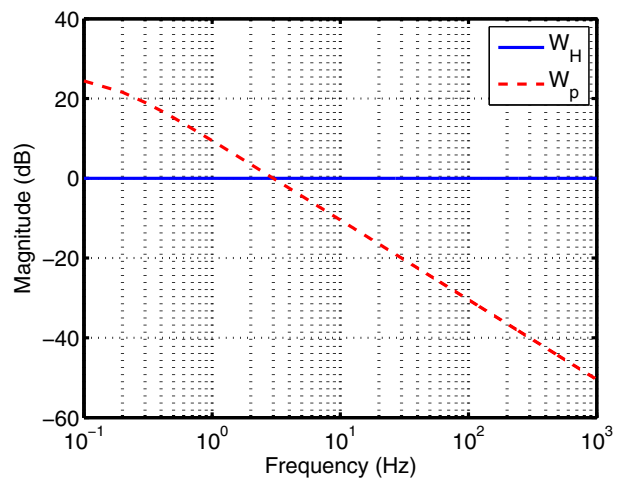


Fig 7. Magnitude responses of the filters W_H and W_p .

The sensor fusion achieved using the H_∞ filtering approach is illustrated by the frequency responses presented in Fig. 8, where the individual transfer functions relate the estimated supply reel velocity with $v_{H,f}$, v , u_m and u_f , and the frequency separation achieved with the designed estimator is clearly visible. At very low frequencies the velocity estimate is mostly determined by the secondary velocity $v_{H,f}$, whereas at high frequencies the estimate is essentially based on the primary velocity v . The reliance of the velocity estimate on the input signals u_m and u_f is determined by the selection of the weight chosen for W_d . A similar formulation can be introduced for the reverse tape motion direction, where the role of the supply reel is performed by the machine reel. The estimated tape velocity at the supply reel can be used jointly with the velocity at the take-up reel measured by the second Hall sensor for the feedback control of the tape transport velocity, as shown in the next section.

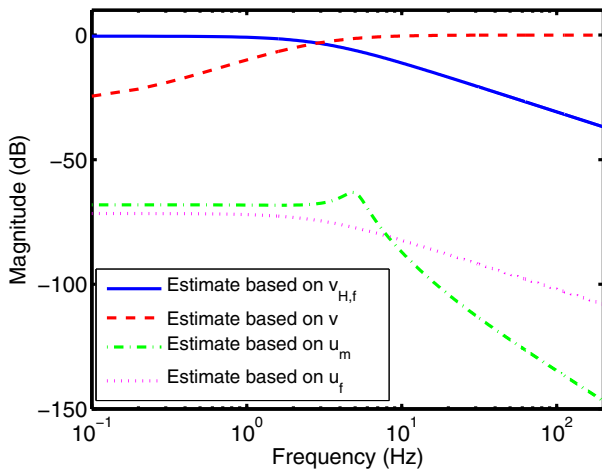


Fig 8. Frequency responses relating the supply reel velocity estimate with the sensor measurements and the input currents.

5. EXPERIMENTAL RESULTS

The performance improvements over a classical tape transport control system, which are obtained by selective feedback of tape velocity information or by estimated velocity information, are illustrated using an experimental tape path. The tape path is determined by the machine and file reels and four roller elements. The rollers are flangeless and guide the tape along the path over the head element. Tension is measured by two strain gauges located on two of the four rollers in the tape path. A picture of the experimental tape transport set-up is shown in Fig. 9.

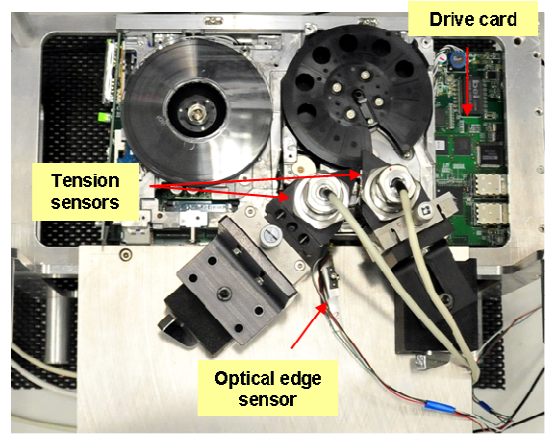


Fig 9. Experimental tape transport set-up.

In Fig. 10 a comparison of the primary tape velocity power spectral densities is given for the three considered control system configurations, namely a) feedback control of supply and take-up reels using primary velocity, b) primary velocity used for feedback control of supply reel and Hall measurement for feedback control of take-up reel, and c) feedback control of the supply reel using the velocity estimated by the two sensors and of the take-up reel using the Hall measurement. The velocity spectrum shows that the main disturbance appears at a frequency of ~ 15 Hz. Note that the two schemes that utilize the Hall velocity information along with the primary velocity achieve reduced velocity variation, especially at the frequencies of the velocity disturbance. In terms of standard deviation of the tape velocity, the three schemes yield a) 5.08 mm/s, b) 3.63 mm/s, and c) 3.57 mm/s.

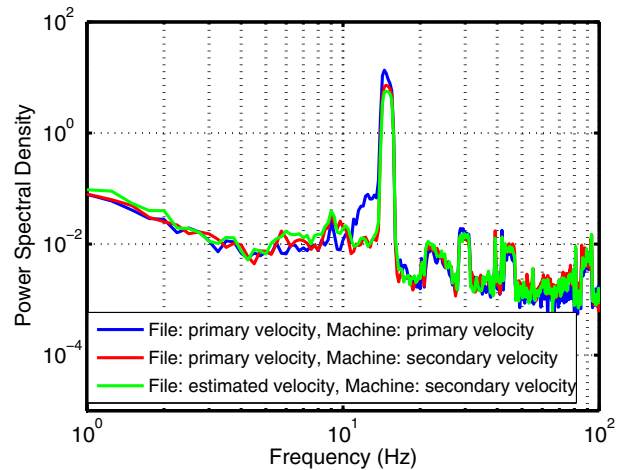


Fig 10. Power spectral density of primary velocity for different tape transport control configurations.

Figures 11 and 12 compare the tape velocity and tension variations obtained by a classical system based on the primary velocity feedback only, and the enhanced system that uses the Hall velocity along with the estimated velocity for the take-up and supply reel, respectively. Note in Fig. 11 the faster converges of the tape velocity in the case where the

Hall measurement is used along with the estimated velocity. Note in Fig. 12 that the improved velocity control provides also an improved performance in terms of tape tension, especially mitigating the disturbances at frequencies close to the tape path resonance. In terms of tension standard deviation, the performance improves from 0.021 N for the system based on primary velocity feedback to 0.016 N for the scheme with the simple switching to the secondary velocity measurement. The tension performance further improves to 0.014 N for the system using joint velocity control.

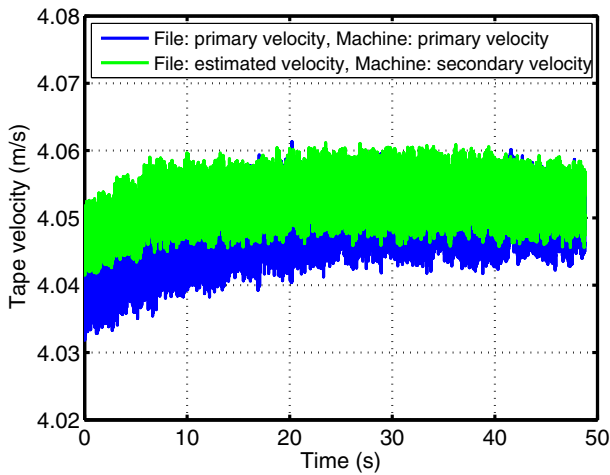


Fig 11. Comparison of tape velocity obtained by feedback of primary velocity only and by joint velocity control.

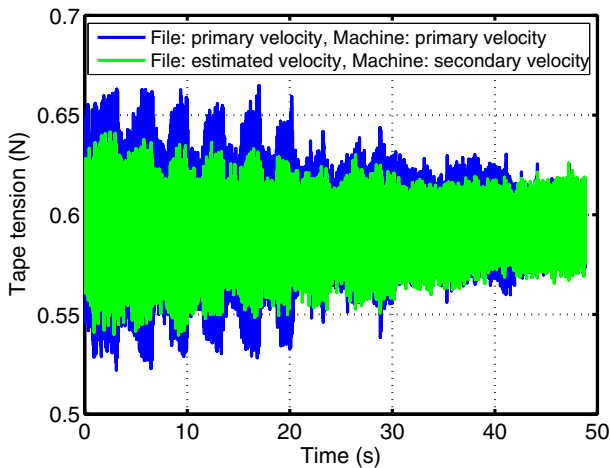


Fig 12. Comparison of tape tension obtained by feedback of primary velocity only and by joint velocity control.

6. CONCLUSIONS

A novel control scheme for tape transport that utilizes velocity measurements from three sources - the Hall sensors yielding secondary velocity information at the tape reels and the servo channel providing primary velocity estimates at the head location - has been introduced. An accurate system model has been derived using an advanced characterization procedure, thereby enabling an optimized two-sensor control

design. H_∞ filtering has been introduced to perform sensor fusion for improved feedback control of the velocity at the two tape reels. Experimental results show improved performance of the novel control concept in terms of reduced velocity variation and tape tension variation when compared with a classical control scheme that only relies on primary velocity feedback. An interesting extension of the concept will be obtained by including feedback of tension variation estimates as well as tension sensor estimates into the tape transport control design.

REFERENCES

- Argumedo A., Berman D., Biskeborn R., Cherubini G., Cideciyan R., Eleftheriou E., Häberle W., Hellman D., Imano W., Jelitto J., Judd K., Jubert P.-O., Lantz M.A., McClelland G.M., Mittelholzer T., Narayan S., and Ölçer S., (2008). Scaling tape-recording areal densities to 100 Gb/in². *IBM J. Res. Develop.*, 52, pp. 513-527.
- Cherubini, G. Cideciyan R.D., Dellmann L., Eleftheriou E., Häberle W., Jelitto J., Kartik V., Lantz M., Oelcer S., Pantazi A., Rothuizen H., Berman D., Imano W., Jubert P.-O., McClelland G., Koeppel P., Tsuruta K., Harasawa T., Murata Y., Musha A., Noguchi H., Ohtsu H., Shimizu O., and Suzuki R., (2011). 29.5 Gb/in² Recording Areal Density on Barium Ferrite Tape. *IEEE Trans. Magn.*, 47, No. 1, pp. 137-147.
- Cherubini, G., Pantazi, A., and Jelitto, J. (2013). Identification of MIMO Transport Systems in Tape Drives. *Proc. 2013 IEEE/ASME International Conference on Advanced Intelligent Mechatronics "AIM 2013,"* pp. 597-602. Wollongong, Australia.
- IDC (2012). THE DIGITAL UNIVERSE IN 2020: Big Data, Bigger Digital Shadows, and Biggest Growth in the Far East, Available: <http://www.emc.com/collateral/analyst-reports/idc-the-digital-universe-in-2020.pdf>
- INSIC (2012). INSIC's 2012-2022 International Magnetic Tape Storage Roadmap, Technology Overview, Available: <http://www.insic.org/news/2012Roadmap/PDF/21%20Roadmap%20-%20TechOverview%20V4.1.pdf>
- Mathur, P. D., and Messner, W. C. (1998). Controller development for a prototype high-speed low-tension tape transport. *IEEE Trans. Control Syst. Technol.*, vol. 6, pp. 534-542.
- Pantazi, A., Sebastian, A., Cherubini, G., Lantz, M., Pozidis, H., Rothuizen, H., and Eleftheriou, E. (2007). Control of MEMS-based Scanning-probe Data Storage Device. *IEEE Trans. Control Syst. Technol.*, vol. 15, no. 5, pp. 824-841.
- Reine, D. and Kahn, M. (2010). "In search of the long-term archiving solution - tape delivers significant TCO advantage over disk," *Clipper Notes*. Available: <http://www.clipper.com/research/TCG2010054.pdf>
- Sebastian, A., and Pantazi, A. (2012). Nanopositioning With Multiple Sensors: A Case Study in Data Storage. *IEEE Trans. on Control Syst. Technol.*, vol. 20, no. 2, pp. 382-394, 2012.